Plasma treatment to improve the adhesion between ABS and PA6 in hybrid structures produced by injection overmolding

Boros R., Ageyeva T., Golcs Á., Krafcsik O. H., Kovács J. G.

Polymer Testing 106 (2022) 107446

Contents lists available at ScienceDirect

Polymer Testing

journal homepage: www.elsevier.com/locate/polytest

Plasma treatment to improve the adhesion between ABS and PA6 in hybrid structures produced by injection overmolding

Róbert Boros [a,b], Ageyeva Tatyana [a,b], Ádám Golcs [c], Olga H. Krafcsik [d], József Gábor Kovács [a,b,*]

[a] Department of Polymer Engineering, Faculty of Mechanical Engineering, Budapest University of Technology and Economics, Műegyetem rkp. 3, H-1111, Budapest, Hungary
[b] MTA-BME Lendület Lightweight Polymer Composites Research Group, Műegyetem rkp. 3, H-1111, Budapest, Hungary
[c] Department of Organic Chemistry and Technology, Budapest University of Technology and Economics, Műegyetem rkp. 3, H-1111, Budapest, Hungary
[d] Department of Atomic Physics, Faculty of Natural Sciences, Budapest University of Technology and Economics, Műegyetem rkp. 3, H-1111 Budapest, Hungary

ARTICLE INFO

Keywords:
Overmolding
Plasma
Photoelectron spectroscopy
Adhesion

ABSTRACT

In this article, we investigate the possibility of combining ABS and PA6 in one structure by means of injection overmolding. The combination of these polymers in one structure is very promising, as PA6 offers good mechanical performance and high melting temperature and abrasion resistance. In contrast, ABS offers excellent impact properties, high water resistance, and cost competitiveness. However, these polymers are incompatible and do not adhere to each other. This study proposes atmospheric plasma treatment to create bonding between ABS and PA6 processed by injection molding. We demonstrated that bonding was created between ABS and PA6 due to the hydroxylation and the chemical conversion of nitrile groups to amide and carboxyl acid after the plasma treatment of ABS. Therefore, the plasma-treated ABS surface enabled the formation of various *H*-bonds, and the strong coupling of ABS and PA6 via secondary chemical binding forces appears. These results were also proved by mechanical tests, which showed that the bonding strength of the ABS/PA6 material pair reaches 12 MPa after plasma treatment, while an untreated case demonstrated no bonding at all.

1. Introduction

Nowadays, innovations in plastic production often arise from the combination of different techniques or different materials within the production of one part. Such integration offers more design freedom to engineers [1], improves the structural performance and aesthetics of plastic parts, and even enables the customization of mass production [2]. One of the most developed manufacturing processes that allow the pairing of two materials in one part without the necessity to use traditional joining methods is two-component injection molding, which is also known under the name "overmolding". This technique is widely used for the production of plastic parts, where the combination of rigid and soft materials or color difference is necessary [3]. Recently, injection overmolding has been more and more used to produce parts that exhibit high structural performance and aesthetic appearance at the same time. This often requires a combination of polymers with entirely different properties that are often considered incompatible. A promising combination of materials is polyamide-6 (PA6) and acrylonitrile butylene styrene (ABS). PA6 has good mechanical performance, high melting temperature, wear, and abrasion resistance, while ABS demonstrates excellent impact properties, high water resistance, and cost competitiveness (Fig. 1) [4].

Despite the attractiveness of the combination of ABS and PA6, these two polymers are incompatible by their nature [5]: PA6 is a semi-crystalline polymer while ABS is amorphous, they have considerably different chemical formulas and different values of T_g (55 °C [6] and 105 °C [7], respectively) and T_m. Czvikovszky et al. [8] discuss the compatibility of a two-component system if the free energy change due to mixing is negative, and the system is transferred to a more stable, lower energy state. In the case of ABS and PA6, these conditions are not fulfilled, and the two materials are incompatible. These facts make ABS and PA6 impossible to pair via fusion-bonding techniques, such as overmolding.

Generally, the adhesion between two polymers forms due to the interatomic and intermolecular interaction at the interface [9]. It is a complex phenomenon of an interdisciplinary character. According to

* Corresponding author. Department of Polymer Engineering, Faculty of Mechanical Engineering, Budapest University of Technology and Economics, Műegyetem rkp. 3, H-1111, Budapest, Hungary.
E-mail address: kovacs@pt.bme.hu (J.G. Kovács).

https://doi.org/10.1016/j.polymertesting.2021.107446
Received 24 September 2021; Received in revised form 8 November 2021; Accepted 18 November 2021
Available online 2 December 2021

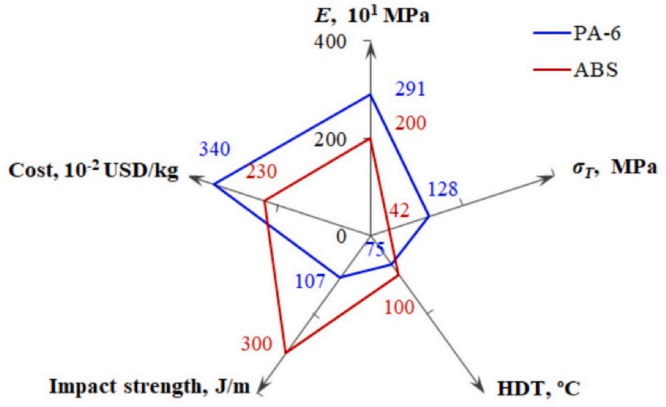

Fig. 1. Comparison of the properties of PA6 and ABS (E – Young modulus, σ_T – tensile strength).

our current understanding, adhesion between two polymers occurs due to the following mechanisms: mechanical interlocking, molecular diffusion, electrostatic interaction, wetting, chemical bonding, and the formation of a weak boundary layer [10]. These mechanisms act simultaneously, but the degree of their impact on the resulting bonding strength depends on the nature of the paired materials and the processing parameters of joining.

As adhesion is a surface phenomenon, it is possible to improve it by means of different surface modification methods. All surface modification methods can be classified into three groups: physical, chemical, and mechanical (Fig. 2). Mechanical surface modification methods are based on the mechanical interlocking theory of adhesion, which states that bonding occurs due to the penetration of the adhesive into pores, cavities, and other irregularities in the substrate surface, forming mechanical anchoring [11]. Consequently, surface roughness plays an important role in bonding.

The "chemical" group of methods are based on mechanical interlocking, wetting, and chemical bonding theories. The purpose of chemical surface treatment of polymers is usually to generate a certain surface roughness or to apply highly oxidizing reagents to enhance adhesion through the formation of polar groups [13]. Several studies investigate the chemical grafting of reactive species on the polymer surface, thus making it possible to join incompatible polymers [14,15].

The "physical" group of methods mainly modify the free energy of a surface (by means of UV/ozone irradiation [16–18], laser [19–21], ion-beam irradiation [22], plasma [23–26], and other methods). The purpose of physical treatment is to remove surface contaminants, trigger oxidation processes, and increase the polarity and wettability of the surface of a polymer [27]. One of the most industrially adapted surface modification methods for polymers is plasma treatment, which can influence the polymer in four ways: etching, crosslinking, the deposition of active chemical species, and the functionalization of the surface. The functionalization of the polymer surface with plasma is of particular interest, as most non-expensive, mass-produced commodity plastics, such as polyethylene (PE), polypropylene (PP) and polystyrene (PS) belong to the polyolefin group, which are inert and do not contain any functional groups, which could promote adhesion.

In industry, the plasma treatment of polymers is widely used to facilitate the application of coatings, paints, sealants, and also to increase the strength of adhesively bonded joints. Two kinds of plasma treatment are currently used for polymers: low-pressure and atmospheric plasma. Low-pressure plasma treatment mostly creates hydroxyl (-OH) and carboxyl (-COOH) polar groups on the non-polar polymer surface, thus increasing the surface energy and wettability, and consequently the adhesion capability of polymers [28]. Atmospheric plasma treatment does not require the creation of low pressure, and therefore it is a highly versatile, easy-to-implement, and inexpensive method of surface activation.

Kubota et al. [29] proved with XPS spectra that after the atmospheric and low-pressure oxygen plasma treatment of polypropylene (PP) and polystyrene (PS) films, carboxyl, carbonyl, and hydroxyl functional groups appear in the surfaces of these polymers. These functional groups facilitate the adhesion of PP and PS. Slavicek et al. [30] examined the influence of atmospheric plasma treatment on the surface of ABS. They found that the plasma treatment of ABS decreased the water contact angle from 94.7° for the reference sample down to 40°. Frascio et al. [31] also found a substantial decrease of a contact angle (from 90° down to less than 10°) for the plasma-treated ABS. De Armentia et al. [32] found that the adhesion strength between ABS and PU painting increases 10-fold after atmospheric plasma treatment. Pizzorni et al. [33] compared the effectiveness of three surface treatment methods (solvent degreasing, abrasion, and low-pressure plasma) for the bonding improvement in adhesively-bonded composites with nylon-6 matrix. The authors proved the oxidative effect of plasma with XPS analysis. They found that low-pressure plasma treatment increases bonding strength nearly three times higher than abrasion and degreasing. Mandolfino et al. [34] proved that cold plasma treatment led to less crack propagation and better joint aging resistance in adhesively-bonded PA6 samples. Although atmospheric plasma treatment is widely used to improve adhesion between polymers and different kinds of coatings or paintings [30,35], the use of atmospheric plasma to improve the bonding formed during overmolding is much less researched. Moritzer et al. [36] developed inline plasma surface modification integrated into injection molding. They created an experimental setup, which consisted of an injection mold with a stationary mounted plasma jet. The authors proved that this setup can effectively increase the surface energy of various engineering plastics and their combinations, such as Polybutylene Terephthalate (PBT)/Acrylonitrile Styrene Acrylate (ASA) and

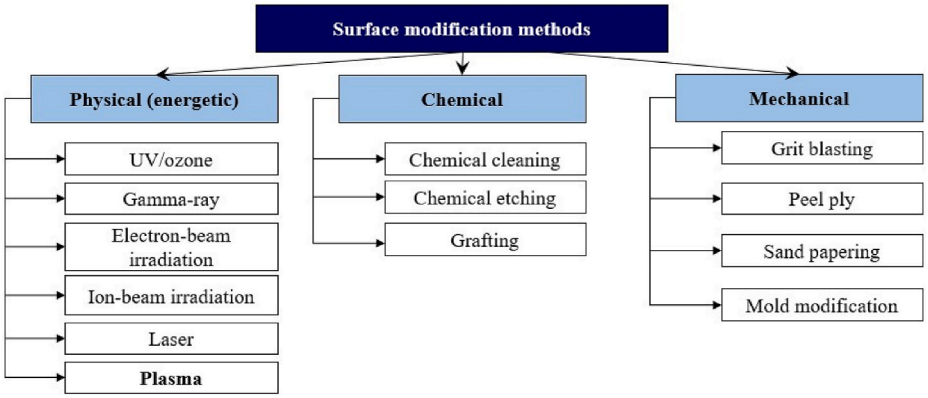

Fig. 2. The Classification of the surface modification methods of polymers (based on [12]).

Table 1
Properties of the materials for examination.

Material	ABS Terluran GP35	PA6 Durethan B30S
Drying temperature and time	80 °C for 4 h	80 °C for 2–6 h
Recommended melt temperature range	220–280 °C	260–280 °C
Recommended mold temperature range	30–60 °C	80–100 °C

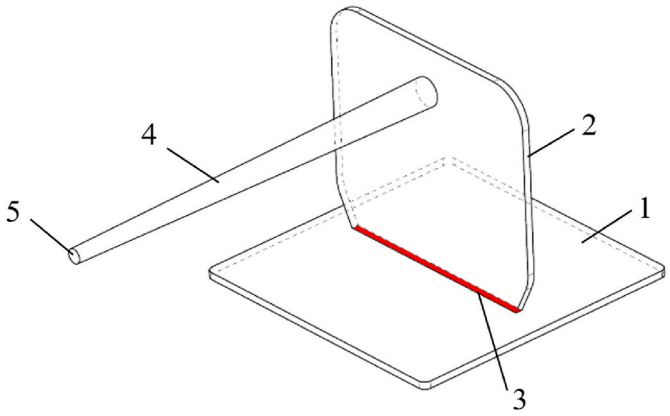

Fig. 3. T-shape test specimen: 1 – base plate; 2 – overmolded rib; 3 – interface (contact surface); 4 – sprue; 5 – injection point.

Polycarbonate (PC)/ABS. However, the PA/ABS combination was not studied. Moreover, the authors mostly concentrated on developing the equipment, while the mechanism of bonding was beyond the scope of their research.

In our research, we investigated how the bond strength between the base plate and the overmolded rib is influenced by the surface properties of the base plate during overmolding (e.g., surface roughness and surface activity). Our study examines surface roughness and the influence of atmospheric plasma treatment on the bonding strength formation during injection overmolding. We investigated several material pairs: ABS/ABS, PA6/PA6, and ABS/PA6. The last pair of materials is considered incompatible, and there is typically no adhesion between them.

2. Experimental

2.1. Production of specimens

We used neat amorphous ABS Terluran GP35 (BASF, Germany, Ludwigshafen) and neat and black semi-crystalline PA6 Durethan B30S (Lanxess, Germany, Cologne) for injection molding and overmolding. Both materials were dried according to the producer's recommendations (Table 1).

For the characterization of the bonding strength between a base plate and an overmolded element, we designed a so-called "T-shape geometry" (Fig. 3). This test specimen consists of an 80 mm × 80 mm × 2 mm base plate (or substrate), which we manufactured separately by conventional injection molding, and a 70 mm × 63 mm × 2 mm rib, which was overmolded onto the base plate. As a result, a contact surface or an interface (Fig. 3 (3)) was formed between the base plate and the rib. The nominal dimensions of the contact area between the base plate and the rib were 60 mm × 2 mm excluding the shrinkage.

We produced eight sets of T-shaped specimens, which differ in the material combinations and whether the base plate was plasma treated or not. The properties of the specimens are listed in Table 2. For the designation of the specimens, we used the format "base plate material/rib material", and the small letter after the base plate material indicates plasma treatment or the lack of it ("u" stands for "untreated" and "t" stands for "treated"). We also produced "one-piece" T-shaped specimens as references for each measurement series. We produced ten specimens for each set.

Table 2
The sets of specimens produced for plasma treatment.

The structural part of the specimen		Overmolded rib	
		PA6	ABS
Base plate	PA6 untreated	PA6-u/PA6	PA6-u/ABS
	PA6 treated	PA6-t/PA6	PA6-t/ABS
	ABS untreated	ABS-u/PA6	ABS-u/ABS
	ABS treated	ABS-t/PA6	ABS-t/ABS

Table 3
The mold surface roughness for the sets of specimens for the surface roughness investigation.

Mold insert	R_a,μm	SD, μm	R_z, μm	SD, μm
polished	0.03	0.01	0.27	0.11
fine sparked	2.86	0.64	15.24	2.77
rough sparked	11.53	1.48	50.00	3.91

Table 4
Injection molding processing parameters for the materials used.

Processing parameter	ABS	PA6
T_{mold}, °C	40	80
T_{melt}, °C	220, 240, 260, 280	240, 250, 260, 270, 280, 290, 300

We produced the specimens on an Arburg Allrounder 370 S 700 290 (ARBURG Holding GmbH, Lossburg, Germany) injection molding machine. The specimens were manufactured in two steps, and each step needed a separate mold. Thus, for the first step (manufacturing of the base plate), we used a conventional two-cavity cold runner injection mold. For the second step (overmolding), we used a specially developed mold equipped with a mechanically operated slider to accommodate the base plate.

To investigate the effect of surface roughness, we used a special injection mold to produce a base plate with different surface roughnesses (with a polished, a fine sparked, and a rough sparked mold insert). For this series of experiments, we chose the amorphous ABS as it has good flowability and low shrinkage. To be able to compare the surface roughness of the base plates, we measured the surface roughness (Ra, Rz) of the mold inserts (EN ISO 4287 [37]) before injection molding using a stationary surface roughness tester (Mitutoyo SJ-400, Mitutoyo, Japan). The results of the measurement of surface roughness are presented in Table 3.

For all the sets of specimens (Table 2), the base plates and the overmolded ribs were manufactured with the mold temperature and melt temperature settings recommended by the material manufacturer. We injection-molded ABS parts by conventional injection molding with melt temperatures from 220 °C to 280 °C and a mold temperature of 40 °C (Table 4). In the case of PA6, we used a melt temperature from 200 °C to 260 °C and a mold temperature of 80 °C. For each set listed in Table 2, we produced 12 specimens.

We used plasma treatment for some of the base plates immediately (not more than 30 s) before the second step of the production of the T-shape specimens — overmolding. The plasma treatment was performed with an FG 5001 plasma generator (Plasmatreat GmbH, Steinhagen, Germany) (Fig. 4 (8)). The plasma was generated from compressed air, the pressure of which was reduced to the desired level by a pressure regulator (Fig. 4 (6)). The compressed air with the reduced pressure was introduced into a Plasmatreat RD1004 rotating plasma head (Fig. 4 (1)).

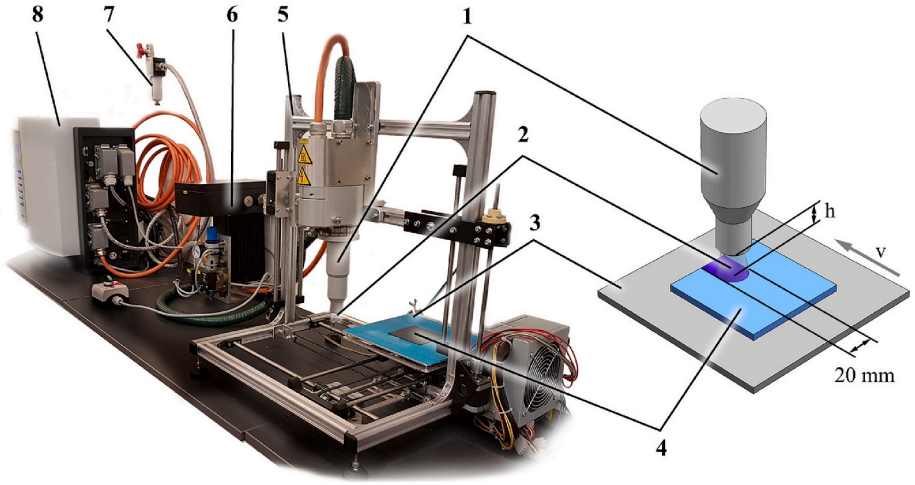

Fig. 4. Plasma treatment setup: 1 – plasma head, 2 – plasma, 3 – support plate, 4 – base plate (*h*: distance from the plasma head to the treated base plate, *v*: the linear speed of the support plate/e.g. plasma treatment speed), 5 – machine moving frame, 6 – pressure regulator, 7 – compressed air, 8 – plasma generator.

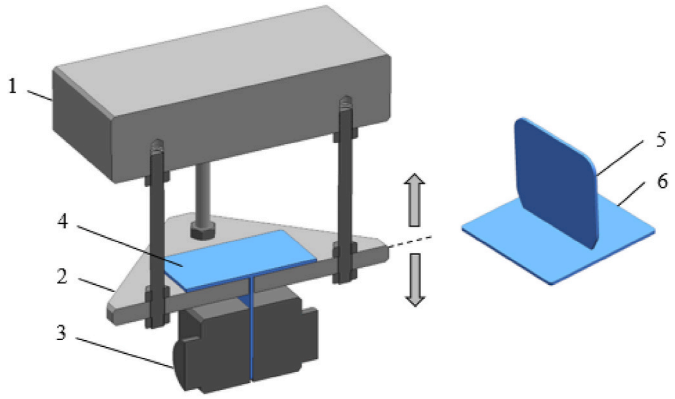

Fig. 5. Test setup of the base plate and rib for measuring bonding strength between the base plate and an overmolded rib (1 – tensile machine, 2 – support plate, 3 – vice-jaw, 4 – specimen, 5 – rib, 6 – base plate).

The parameters affecting the plasma properties (voltage, amperage) were set on the control unit. The plasma head was mounted on a frame (Fig. 4 (5)). The prefabricated base plates (Fig. 4 (4)) were fixed on the support plate (Fig. 4 (3)). The movement of the support plate was controlled by a computer.

Plasma treatment was carried out with compressed air at a pressure of 3.5 bar, a voltage of 280 V, and a current of 17.5 A. The central 20 mm wide band of the preform was treated by moving the support plate with a speed of 1000, 3000, and 6000 mm/min under the plasma head (hereafter, we will call this speed "plasma treatment speed"). The vertical distance between the plasma head and the moving table varied from 2 to 10 mm.

2.2. Mechanical testing

To define the bonding strength between the base plate and the overmolded rib, we performed tensile tests with a Zwick Z020 universal tensile testing machine (Zwick Roell AG, Ulm, Germany) with the load cell limit of $\pm$20 kN. We developed a special grip (Fig. 5) to fix the T-shape test specimen during the tensile test, where the rib is fixed with the clamp, and the base plate is laid on a plate with a gap. The gap is 1 mm larger than the rib on each side. The connecting surface of the preform and the rib is 120 mm^2. All the tensile tests were performed at room temperature and relative humidity of 50%. The testing speed was 5 mm/min, and we tested ten specimens for each combination of materials.

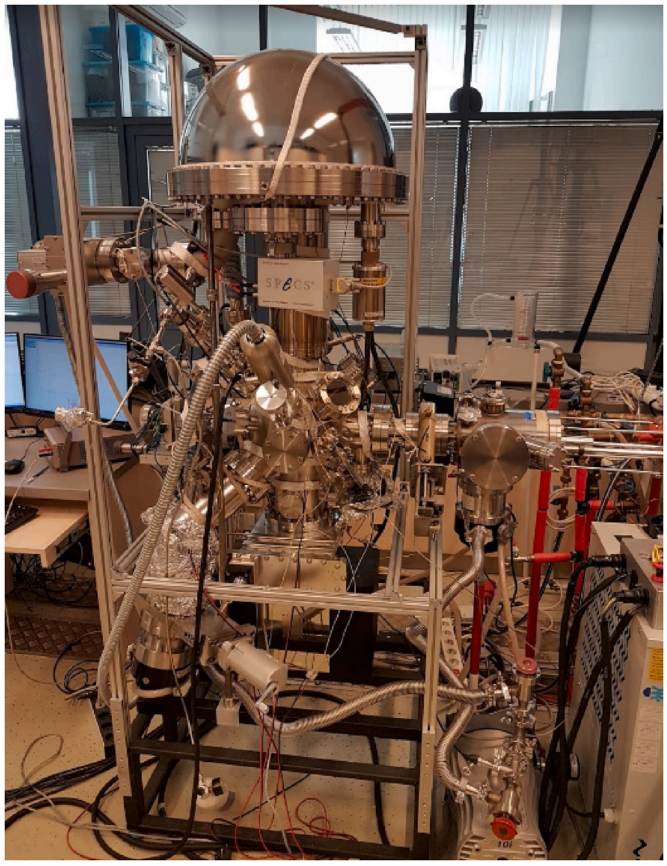

Fig. 6. Complex XPS-SAM equipment used for XPS.

2.3. X-ray photoelectron spectroscopy (XPS)

To examine the surfaces of the overmolded samples, we performed X-ray Photoelectronic Spectroscopy (XPS) with a twin anode X-ray source (XR4, Thermo Fisher Scientific, Waltham, Massachusetts, USA) and a hemispherical energy analyzer with a nine-channel Multi-Channel Detector Phoibos 150 MCD (SPECS, Berlin, Germany) (Fig. 6). The base pressure of the analysis chamber was around 2×10^{-9} mbar. We

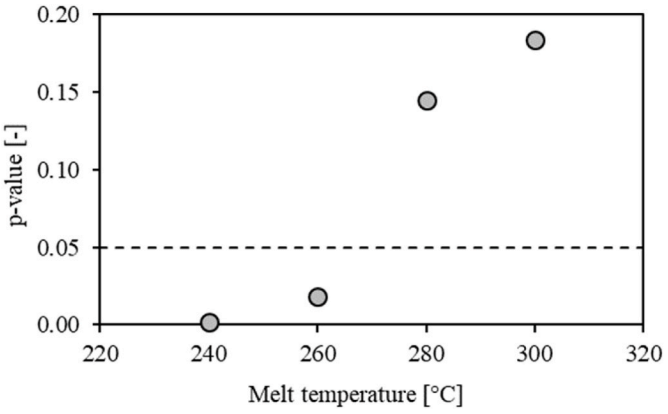

Fig. 7. Variation of ANOVA p-value as a function of melt temperature.

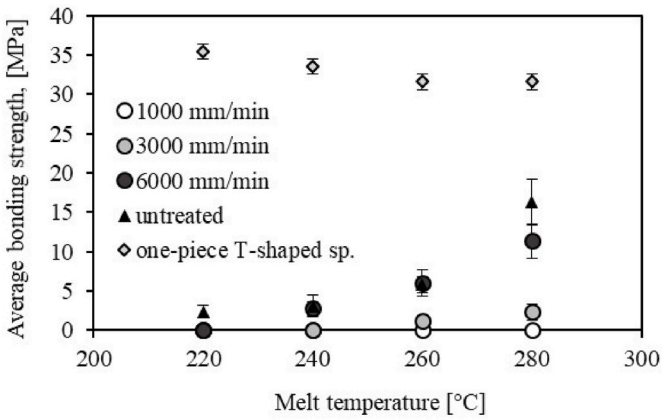

Fig. 8. Variation of the average strength of the bond in ABS-u/ABS, and ABS-t/ABS specimens (treated at different plasma speed settings) as a function of the melt temperature.

analyzed the samples with an Mg K_α anode (1253.6 eV) without monochromatization. Low-resolution spectra were recorded in the range of 0–1100 eV, and high-resolution spectra were taken in the range of 300 to 280 eV in the case of the C-1s photoelectron peak and 410-394 eV in the case of the N-1s photoelectron peak. The peaks were fitted with the CasaXPS software. The binding energies correspond to the C-1s photoelectron peak of C–C bonds and C–H bonds (hydrocarbon contamination) at 285.0 eV. The sensitivity of the measurement was 0.1 at%.

To evaluate the effect of plasma treatment on bonding, we examined the polarizability of ABS and PA6 with and without plasma treatment. We estimated molecular polarizability and the polar surface area with the Polarizability Plugin® and Polar Surface Area 2D Plugin® (both from ChemAxon, Budapest, Hungary). For polarizability calculations, we used the atomic parameters reports by Miller and Savchik [38] in addition to those reported by Jensen [39]. For the estimation of topological polar surface area (TPSA), we used the method described by Ertl et al. [40].

2.4. Contact angle measurement

To examine the wettability of the samples, we used contact angle measurements with the Drop Shape Analyser Krüss DSA 30 (Krüss, Germany, Hamburg). We measured the contact angle of the water drop immediately after the plasma treatment of polymer samples. We used 10 μl millipore water for the tests. We measured the contact angle on three drops/specimens. The room temperature was 25 °C, and humidity was 80% in the measuring cell.

3. Results and discussion

3.1. Influence of the surface roughness of the base plate on bonding

First, we investigated whether the surface roughness of the base plate changes with mold surface roughness with different process parameters. The investigated process parameters are melt temperature (220, 240, 260, 280 °C), mold temperature (40, 60, 80 °C), and holding pressure (150, 300, 450 bar). Holding time was 4 s, and residual cooling time was 15 s. After injection molding, the base plates were stored at room temperature at 50% relative humidity, and 4–6 h later, their surface roughness (Ra, Rz) was measured. We found that neither melt or mold temperature nor holding pressure significantly affected the surface roughness of the base plates. Therefore, in the further steps of the experimental series, the base plates were produced with a melt temperature of 240 °C, a mold temperature of 60 °C, and a holding pressure of 450 bar and with the three different mold inserts: polished, fine sparked, and rough sparked.

We injection molded the ribs onto the base plate with different melt temperatures (220, 240, 260, 280, and 300 °C). Specimens manufactured at the lowest melt temperature did not bond at all. For the higher temperatures, the average tensile strength increased with melt temperature with a saturation characteristic for all three surface roughnesses. We performed ANOVA (analysis of variance) to evaluate the influence of surface roughness on bonding strength for each melt temperature group. At a 95% significance level, we proved that the surface roughness affects bond strength at low melt temperatures, while it does not affect bond strength at higher melt temperatures (Fig. 7). At high melt temperatures, the melt arrives at the base plate, heats the base plate above its melt temperature, and forms a proper weld. At low melt temperatures, that cannot happen. Therefore the contact area, thus surface roughness, plays a key role in the bond between the plate and the rib.

3.2. Influence of plasma treatment on bonding

We investigated other surface treatment possibilities as surface roughness cannot offer an overall solution to bonding problems.

3.2.1. Mechanical test results

3.2.1.1. The effect of plasma treatment on the joining of the ABS base plate and an overmolded ABS rib. We examined the influence of two processing parameters on the bonding strength of the ABS/ABS material pair. The first parameter was the melt temperature of ABS during the ovemolding stage, which varied from 220 to 280 °C with steps of 20 °C. The second parameter was plasma treatment speed which was 1000, 3000, and 6000 mm/min. We used one-piece T-shape specimens produced with one-shot injection molding as reference. In the case of the ABS-u/ABS specimens, average bonding strength increased with increasing melt temperature, reaching its maximum of ~16 MPa when the melt temperature of the overmolded ABS was 280 °C (Fig. 8). We found that plasma treatment in the case of ABS/ABS does not cause any improvement in bonding strength. Even at the plasma speed of 1000 and 3000 mm/min, bonding strength was lower than for the untreated samples at each melt temperature. In the case of 6000 mm/min plasma treatment speed, average bonding strength was the same as that of the ABS-u/ABS samples for all the temperatures except the highest temperature, where the ABS-t/ABS specimens demonstrated lower bonding strength than the untreated specimens. We concluded that in the case of the ABS/ABS combination, plasma treatment leads to the decrease of bonding strength between a base plate and an overmolded rib. This is because of the apolar nature of ABS. The more we treated ABS with plasma, the more polar its surface became. This caused a polarity incompatibility of the treated and untreated ABS elements. We will further discuss this issue in more detail in Section 3.3.

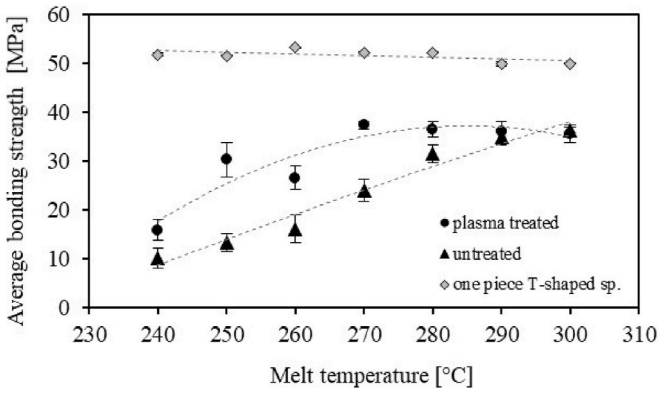

Fig. 9. Variation of the average strength of the bond in PA6-u/PA6, and PA6-t/PA6 specimens as a function of melt temperature (Note that plasma treatment speed was 6000 mm/min).

3.2.1.2. The effect of plasma treatment on the joining of a PA6 base plate and an overmolded PA6 rib. For the PA6/PA6 material pair, we treated base plates with plasma at a speed of 6000 mm/min, and then we overmolded the ribs at different melt temperatures (Fig. 9). We found that in the case of PA6-u/PA6 specimens, the average tensile strength reached its maximum of 36.32 ± 0.56 MPa at a melt temperature of 300 °C.

Plasma treatment significantly improves the bonding for the PA6/PA6 material pair (especially at temperatures lower than 280 °C). This phenomenon can be explained by the polar nature of PA6, which is even further increased by the plasma treatment. The highest bonding strength for PA6-t/PA6 specimens reaches almost 75% of that of the one-piece part.

3.2.1.3. Effect of plasma treatment on the joining of a PA6 base plate and an overmolded ABS rib. We produced PA6 base plates and overmolded ABS ribs on them. The melt temperature of ABS was 260 °C. We observed no bonding between the PA6 base plate and the ABS overmolded rib in both cases – with and without plasma treatment (Fig. 10). We treated the PA6 base plates at different speeds (200, 1000, 2000, 4000, 6000 mm/min) and with the distance between the base plate and plasma source equal to 8 mm. Even the slowest plasma treatment speed (i.e., longest treatment time) did not increase the adhesion in PA6-t/ABS specimens. Later we will explain this phenomenon with the XPS test results.

3.2.1.4. Effect of plasma treatment on the joining of an ABS base plate and an overmolded PA6 rib. In this section, we report the results of the influence of the plasma treatment and overmolding processing parameters on the bonding between an ABS base plate and a PA6 rib. We examined the influence of melt temperature during overmolding, as well as the influence of the speed of plasma treatment and the distance between the plasma source and the treated surface.

A PA6 rib was overmolded onto a base plate made of ABS. Melt

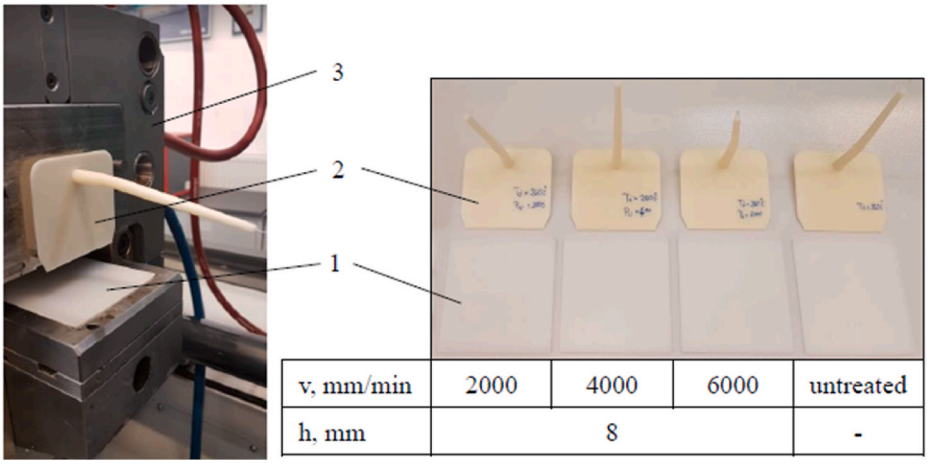

Fig. 10. PA6/ABS specimens, untreated and with plasma treatment (1 – PA6 base plate; 2 – ABS overmolded rib; 3 – injection mold).

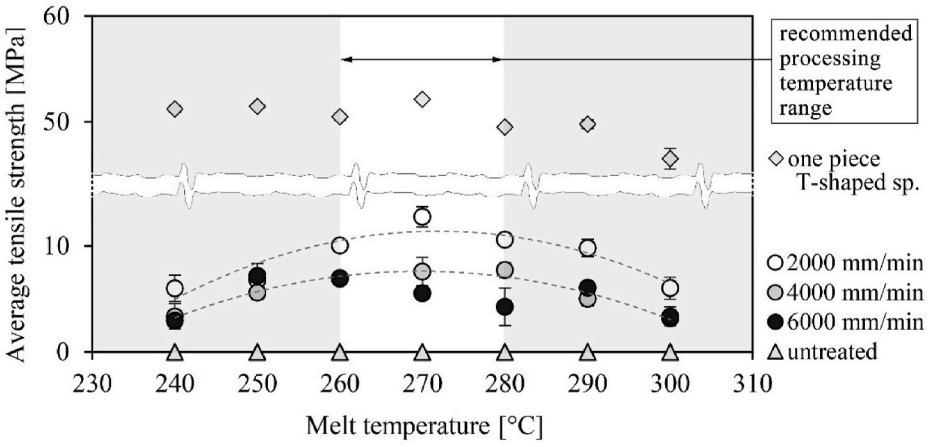

Fig. 11. Variation of average bonding strength of the joint in ABS/PA6 specimens (note, that here the reference is a one-piece PA6 specimen).

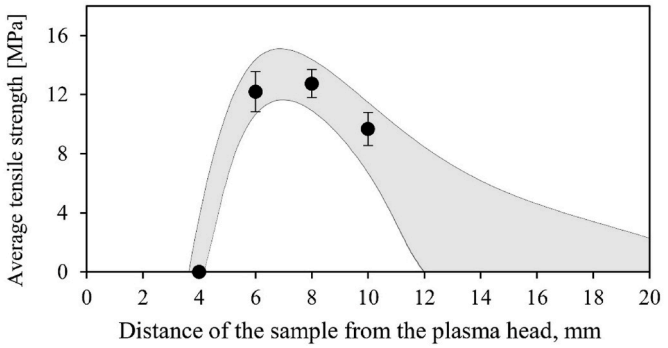

Fig. 12. Variation of the average bonding strength of the joint in ABS/PA6 specimens depending on the distance of the treated base plate from the laser source (Note that the linear speed of the support plate v = 2000 mm/min). We expected a Weibull-like function and based on the parameters we had, the expected range for the measured points were highlighted with the grey area.

Table 5
Summary of the effect of plasma treatment on bonding strength for the different combinations of ABS and PA6.

The structural part of the specimen		Overmolded rib	
		PA6	ABS
Base plate	PA6-u	36.32 ± 0.56 MPa	No bonding
	PA6-t	37.26 ± 0.81 MPa	No bonding
	ABS-u	No bonding	16.31 ± 2.87 MPa
	ABS-t	12.76 ± 0.95 MPa	11.34 ± 2.19 MPa

temperature was varied from 240 to 300 °C with a step of 10 °C. We observed no bonding in the case of ABS-u/PA6 specimens. After plasma treatment at different speeds, bonding between ABS base plates and PA6 ribs appeared. The lower the plasma speed (i.e., the higher the treatment time) was, the stronger bonding was.

We also found that bonding strength depended on the temperature of the overmolded PA6 melt. Thus, the bonding strength in ABS-t/PA6 specimens reached its maximum as a result of plasma treatment at 2000 mm/min and when the melt temperature of PA6 was 270 °C. Moreover, the maximum bonding strength at the same melt temperature was observed at all tested plasma treatment speeds (4000 and 6000 mm/min). This phenomenon indicates that bonding between ABS and PA6, which are considered incompatible polymers, can occur and achieves its maximum if the ABS is treated with plasma prior to overmolding and the overmolded PA6 melt has a temperature of 270 °C.

The maximum achieved bonding strength between ABS and PA6 was 12 MPa, which is roughly four times lower than the strength of a one-piece PA6 part (~50 MPa). However, considering the fact that ABS-u/PA6 specimens do not join at all, plasma treatment offers a huge improvement in coupling these incompatible polymers. Moreover, the decrease of plasma speed from 4000 to 2000 mm/min produces almost

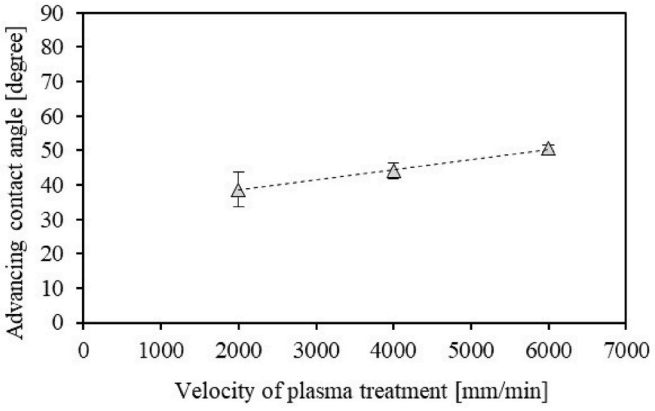

Fig. 14. The variation of the advancing contact angle on the plasma-treated ABS surface as a function of the velocity of plasma (at h = 8 mm).

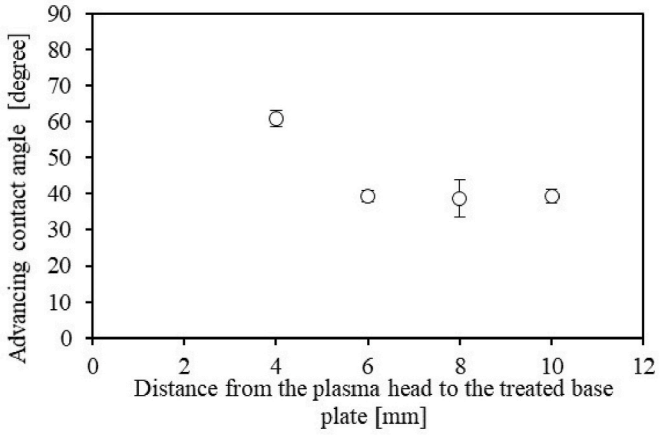

Fig. 15. The advancing contact angle on the plasma-treated ABS surface as a function of the distance of the treated base plate from the plasma head with the linear speed of the support plate of 2000 mm/min.

double the bonding strength between ABS and PA6 at the optimal overmolding melt temperature (Fig. 11).

The influence of the distance between the plasma source and the treated specimen on the bonding strength between ABS and PA6 is much less evident than the influence of plasma speed. We observed that when this distance was 4 mm, no bonding occurred between the materials (Fig. 12). When we increased this distance to 6, 8, and 10 mm, we observed bonding between ABS and PA6.

3.2.1.5. Summary of the mechanical test results. In Table 5, we show the results of the tensile tests for the examined material pairs with treated and untreated base plates. Plasma treatment had no effect in the case of

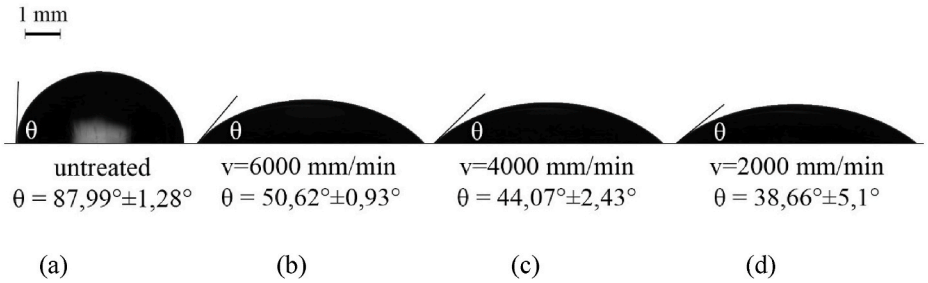

Fig. 13. Advancing contact angle measurements on the ABS surface: (a) untreated, (b) after plasma treatment with the speed of 2000 mm/min, (c) 4000 mm/min; (d) and 6000 mm/min.

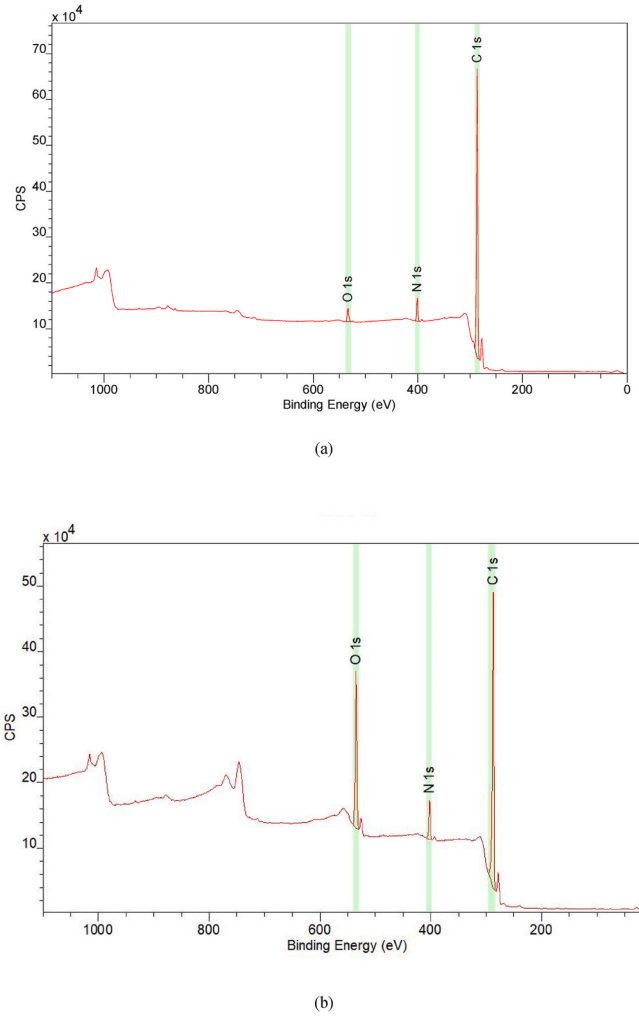

Fig. 16. XPS survey spectra of the (a) untreated and (b) plasma-treated ABS base plate.

PA6-t/ABS specimens and had a negative effect on bonding in ABS-t/ABS specimens. We found that plasma treatment significantly improved bonding in ABS-t/PA6 specimens (there was no bonding without plasma treatment and bonding strength was 12 MPa with plasma treatment).

3.2.2. Contact angle measurement results

The first explanation of the positive influence of the plasma treatment on the bonding between an ABS base plate and a PA6 rib is the increase of the wettability of the treated polymer surface. We examined the wettability of the treated ABS base plate by measuring the advancing contact angle of a water droplet on the polymer surface treated with plasma at different speeds (Fig. 13). We found that for an untreated base plate, the advancing contact angle was 86°, while plasma treatment at a speed of 6000, 4000, and 2000 mm/min decreased the value of a contact angle to 62, 37, and 27°, respectively (Fig. 14).

We measured the contact angle on the treated ABS surface with different distances of the plasma head from the treated surface (Fig. 15). We observed that with 4 mm, the advancing contact angle was 60°, which is lower compared to the untreated base plate (86°) but still too high to ensure bonding. This result correlates well with the results of the mechanical tests, where no bonding was observed when the distance between the plasma head and ABS surface was 4 mm (Fig. 12). The increase of the distance to 6 mm leads to the decrease of the contact angle (~40°). However, a further increase of the distance between the plasma head and the ABS surface does not change the contact angle significantly.

Table 6
Surface elemental composition of untreated and plasma-treated samples.

Base plate	elemental composition, at %			O/C ratio
	C	O	N	
untreated ABS	94.1	2	3.9	2%
plasma-treated ABS	79	15.5	5.5	20%

Table 7
The rate of chemical bonding states of N and C on the surface of the untreated and plasma-treated ABS sample in percentages.

Distribution of bond states, %	N 1s		C 1s		
	R–CN	NH_4^+	C–H/ C–C	R–CN/ C–O–H	R-O-C═O/ N–C═O
without treatment	100	0	84.8	15.2	0
plasma treatment	82.3	17.7	56.8	31.9	11.3

3.2.3. XPS examination results

We carried out the XPS examination of the ABS base plate surfaces in order to determine their chemical composition before and after plasma treatment. The low-resolution spectra of the untreated and plasma-treated ABS specimens are presented in Fig. 16 contains the elemental concentrations of the evaluated surface for both the untreated and plasma-treated ABS. The concentration of O atoms and N atoms increases due to plasma treatment at the expense of the concentration of C atoms which is why we performed a deeper examination (Table 6). We determined the chemical binding states of C and N atoms by fitting the curve of high-resolution C-1s and N-1s photoelectron peaks. The untreated surface of the ABS sample consists of only one N-1s chemical bonding state at 399.8 eV, corresponding to an R–CN bond. For the plasma-treated sample, an additional peak appears at around 402 eV, corresponding to an NH_4^+ bond.

In the case of the untreated ABS plate, the C-1s peak can be fitted by two peaks at 285 eV and at 286.5 eV, corresponding to C–H/C–C bonds and C–OH/R–CN bonds, respectively. It must be noted that the R–CN bond corresponds to 286.3 eV, but it is not possible to separate it from C–OH by deconvolution. In the case of the plasma-treated ABS plates, we identified a third bonding state at 289 eV at the C-1s photoelectron peak, in addition to the chemical bonds corresponding to 285 eV and 286.5 eV. This third peak corresponds to R-O-C═O and C–O–H chemical bonds (Table 7).

From a chemical point of view, ABS has a quite apolar nature with poor polarizability and a lack of hydrogen binding sites (molecular polarizability ~ 30 Å^3, polar surface area ~24 Å^2, *H*-bond donors/acceptors = 0/1). Thus, mainly π-π interactions between the aromatic units and other weak secondary binding forces (e.g., dispersion forces, *van der Waals* forces, π-dipole, and dipole-dipole interactions) predominate between the stereoelectronically complementary molecular groups in the case of ABS/ABS coupling.

By contrast, PA6 has a more polar nature than ABS. In the case of a PA6/PA6 connection, typically, binding is provided by the dipole-dipole interactions among the polymer chains. Moreover, *H*-bonds as the strongest secondary binding forces are also present (*H*-bond donors/acceptors = 1/2), allowing the formation of 2 different *H*-bonds among the polymer chains). Consequently, these stronger PA6/PA6 interactions at the molecular level resulted in increased average tensile strength. The most important molecular interactions for untreated polymers can be seen in Fig. 17.

The plasma treatment significantly affected these interactions by chemically modifying the surfaces of the studied polymers. These modifications are mainly oxidation reactions, especially hydroxylations.

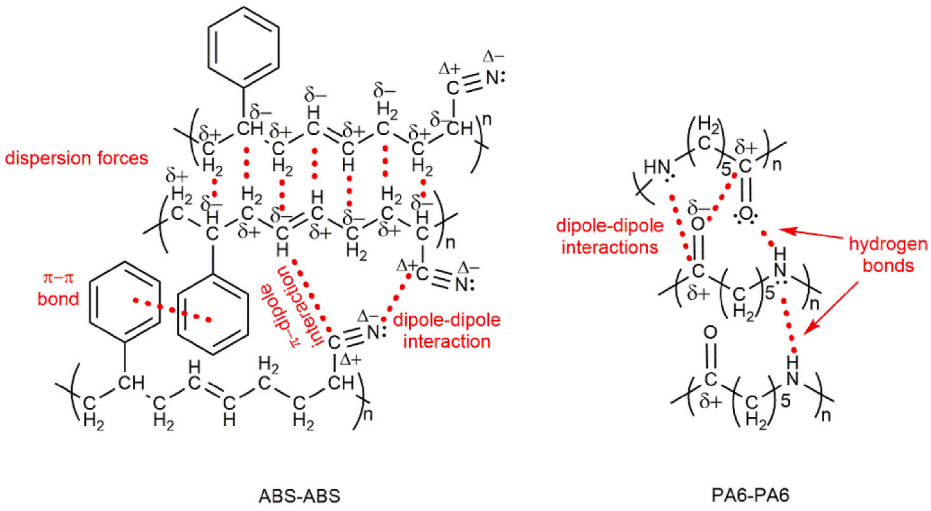

Fig. 17. The main secondary binding forces among polymer chains for ABS/ABS and PA6/PA6 connections without preliminary plasma treatment (the bonds do not indicate exact interactions but schematically show the possibilities for bindings based on the structural properties of the monomer units).

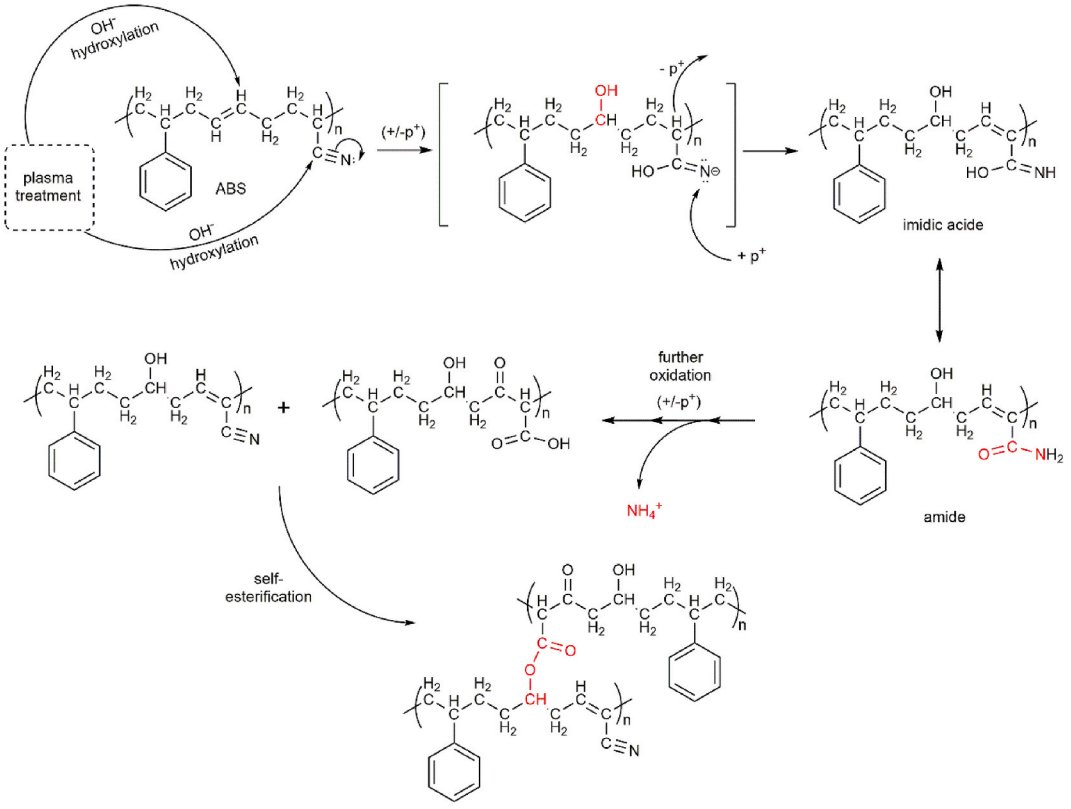

Fig. 18. The supposed mechanism for typical chemical modifications of the surface of ABS by plasma treatment. The new functional groups indicated by XPS are marked in red in the hypothesized molecular structures. (For interpretation of the references to color in this figure legend, the reader is referred to the Web version of this article.)

Thus, the polymer surfaces tend to become increasingly polar due to the plasma. The obtained polarized surface of the plasma-treated ABS induced a polar incompatibility with the untreated surface. It is also supported by the reduced tensile strength of ABS-products if a plasma treatment on one of the specimens was previously applied. In contrast, for PA6/PA6 coupling, plasma showed a weaker but opposite influence on binding properties. Since the untreated polymer was polar as well, the modifications only altered this feature to a lesser extent. On the other hand, the new hydroxyl and oxo groups increase the number of possibilities for establishing additional hydrogen bonds, which can further enhance binding strength. Higher temperatures can provide mobility for polymer chains to be properly arranged, which may enable an increased number of interactions.

ABS and PA6 are totally incompatible due to their different physicochemical nature. Strong interactions, like *H*-bonds, cannot occur, while the formation of other weaker binding forces is also unlikely due to the polar incompatibility. The XPS results show that the plasma is most likely to oxidize the chain saturations and the nitrile groups of the

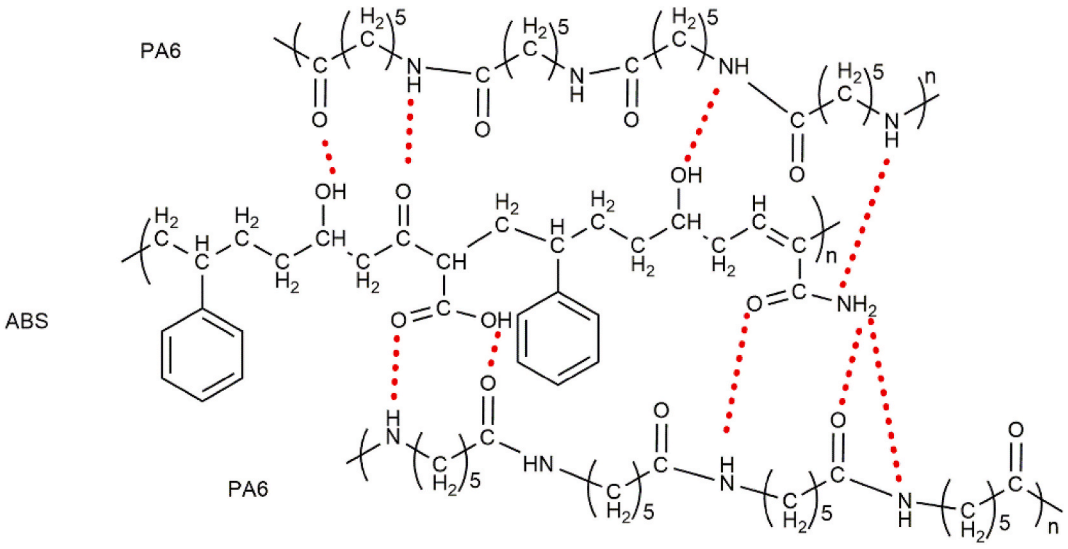

Fig. 19. Possible *H*-bonds between the surface-modified ABS and untreated PA6 (the *H*-bonds do not indicate exact interactions but schematically show the possibilities for bonds based on the number of donor and acceptor groups of the monomer units).

ABS as they are the most reactive centers of the polymer. We suggested the mechanism for chemical reactions induced by plasma treatment based on the XPS results, as shown in Fig. 18 (the plasma treatment can enable various reactions, even those of radical or mixed mechanisms. Thus the reported synthetic pathway represents only one of the possible schemes).

Although the formation of dipole-based interactions is still limited in this case due to the presence of the apolar aromatic units (molecular polarizability ~ 32 $Å^3$ (reflects the altered abilities for dipole-based secondary chemical interactions) and polar surface area ~63 $Å^2$ (reflects the altered polarity-based physical compatibility)), the conversion of the nitrile groups to amide and carboxylic acid in addition to the entering hydroxyl groups significantly increases the potential for the formation of *H*-bridges (*H*-bond donors/acceptors = 3/3). These structural modifications make it possible to form up to nine different *H*-bonds between ABS and PA6, as illustrated schematically in Fig. 19.

Overall, the large number of new *H*-donor and *H*-acceptor sites upon plasma treatment caused a strong binding between the surface-modified ABS and the untreated PA6.

4. Conclusion

We successfully combined two incompatible polymers (ABS and PA6) in one structure by injection overmolding. Bonding between the examined materials was improved with the help of plasma treatment. The main findings of the research are summarized below:

1. The surface roughness of the base plate affects bond strength at low melt temperatures, while it does not affect bond strength at higher melt temperatures.
2. Plasma treatment did not have an effect on the bonding of PA6-t/ABS specimens, and had a negative effect on the bonding of ABS-t/ABS specimens. In contrast, the ABS base plate and the PA6 rib did not bond without plasma treatment, but had a bonding strength of 12 MPa after plasma treatment.
3. The bonding strength between an ABS base plate and a PA6 rib depends on two processing parameters: the melt temperature of the overmolded PA6 and plasma treatment speed. The optimum temperature of the PA6 melt for overmolding was 270 °C. At this temperature, the plasma-treated samples demonstrated maximum bonding strength. We also found that the slower plasma treatment speed was, the higher bonding strength was. The maximum bonding strength between an ABS base plate and an overmolded PA6 rib was 12 MPa, and it was achieved after plasma treatment at 2000 mm/min and when the melt temperature of PA6 was 270 °C.
4. The bonding strength between ABS and overmolded PA6 also depends on the distance between the plasma head and the treated surface. When this distance was 4 mm, no bonding occurred, but when this distance was increased to 6 mm, bonding between ABS and PA6 appeared. However, a further increase of the distance to 8 mm and 10 mm did not have a significant effect on bonding. These results were also proved with contact angle measurements. At a plasma head–ABS surface distance of 4 mm, the contact angle on the plasma-treated ABS surface was 60°, which was lower than on an untreated surface (86°) but still quite high to ensure good bonding. Increasing the distance to 6 mm led to the decrease of the contact angle to 40°. However, a further increase of the distance between the plasma head and the ABS surface did not change the contact angle significantly.
5. We explained the chemical mechanisms of the formation of bonds between the plasma-treated ABS and overmolded PA6 with XPS results. The XPS results showed hydroxylation and the chemical conversion of nitrile groups to amide and carboxyl acid after plasma treatment. Therefore, the plasma-treated ABS surface enabled the formation of various *H*-bonds and the strong coupling of ABS and PA6 via secondary chemical binding forces. Plasma treatment can establish chemical interactions between ABS and PA6 and this way provide strong bonding between them in overmolding.

Funding

This work was supported by the National Research, Development and Innovation Office, Hungary (2019–1.1.1-PIACI-KFI-2019-00205, 2018–1.3.1-VKE-2018-00001, 2017–2.3.7-TÉT–IN–2017-00049). The research reported in this paper and carried out at BME has been supported by the NRDI Fund (TKP2020 NC, Grant No. BME-NC) based on the charter of bolster issued by the NRDI Office under the auspices of the Ministry for Innovation and Technology.

CRediT authorship contribution statement

Róbert Boros: Performing Experiments, Formal analysis, Investigation, Writing. **Ageyeva Tatyana:** Conceptualization, Writing, Validation, Writing – review & editing. **Ádám Golcs:** Investigation, Writing. **Olga H. Krafcsik:** Investigation, Writing. **József Gábor Kovács:**

Supervision, Conceptualization, Resources, Funding acquisition, Review & Editing.

Declaration of competing interest

The authors declare that they have no known competing financial interests or personal relationships that could have appeared to influence the work reported in this paper.

Acknowledgments

We would like to express our special thanks to Gábor Barna from Plasmatreat GmbH. We wish to thank Arburg Hungária Kft. for the ARBURG Allrounder 470 A 1000–290 injection molding machine, Tool-Temp Hungária Kft., Lenzkes Gmbh and Piovan Hungary Kft. for the accessories.

References

[1] R. Boros, P.K. Rajamani, J.G. Kovács, Combination of 3D printing and injection molding: overmolding and overprinting, Express Polym. Lett. 13 (2019) 889–897, https://doi.org/10.3144/expresspolymlett.2019.77.
[2] H.E. Quinlan, T. Hasan, J. Jaddou, A.J. Hart, Industrial and consumer uses of additive manufacturing: a discussion of capabilities, trajectories, and challenges, J. Ind. Ecol. 21 (2017) 15–20, https://doi.org/10.1111/jiec.12609.
[3] G.J. Bex, J.D. Keyzer, F. Desplentere, A. Van Baela, Two-component injection moulding of thermoplastics with thermoset rubbers: process development, AIP Conference Proceedings (2017) 120001, https://doi.org/10.1063/1.5016759, 1914.
[4] H. Singh, Compatibilization of abs/pa6 blends using sagma copolymer: study of the mechanical properties, International Journal of Latest Technology in Engineering VI (2017) 57–63. Management & Applied Science.
[5] G. Pahl, W. Beitz, J. Feldhusen, K.H. Grote, Engineering Design. A Systematic Approach, third ed., Springer-Verlag London Limited, London, 2007.
[6] PlacticFinder, PA6 (Polyamide 6, nylon 6, polycaprolactone, https://www.plasticfinder.it/pa6/pa6-poliammide-6-nylon-6-polycaprolactam. (Accessed 2 November 2021).
[7] PlacticFinder, ABS (Acrylonitrile Butadiene Styrene). https://www.plasticfinder.it/abs/acrilonitrile-butadiene-stirene. (Accessed 2 November 2021).
[8] T. Czvikovszky, P. Nagy, J. Gaál, A Vegyes Polimerhulladékok Újrahasznosításának Termodinamikai Korlátai. Kompatibilizáció. In 'A Polimertechnika Alapjai', Műegyetemi Kiadó, Bupadest, 2007.
[9] C. Poisson, V. Hervais, M.F. Lacrampe, P. Krawczak, Optimization of PE/binder/PA extrusion blow-molded films. Ii. Adhesion properties improvement using binder/eva blends, J. Appl. Polym. Sci. 101 (2006) 118–127, https://doi.org/10.1002/app.22407.
[10] S. Ebnesajjad, Chapter 5 - theories of adhesion, in: second ed., in: S. Ebnesajjad (Ed.), Surface Treatment of Materials for Adhesive Bonding, William Andrew Publishing, Oxford, 2014, pp. 77–91.
[11] M. Benaissaiation, F. Benkhenafou, A. Ziadi, L.B.P. Martinez, F.J. Belzunce, L. Douadji, The effects of shot peening on the surface characteristics of 35ncd16 alloy steel, Period. Polytech. - Mech. Eng. 64 (2020) 199–206, https://doi.org/10.3311/PPme.13229.
[12] M. Hadmi, M.N. Saleh, J.A. Poulis, Improving the adhesion strength of polymers: effect of surface treatments, J. Adhes. Sci. Technol. 34 (2020) 18, https://doi.org/10.1080/01694243.2020.1732750.
[13] Z. Shu, X. Wang, Environment-friendly Pd free surface activation technics for abs surface, Appl. Surf. Sci. 258 (2012) 5328–5331, https://doi.org/10.1016/j.apsusc.2012.01.141.
[14] E.G.R. dos Anjos, J. Marini, L.S. Montagna, T.L. do Amaral Montanheiro, F. R. Passador, Reactive processing of maleic anhydride-grafted abs and its compatibilizing effect on PC/ABS blends, Polymer: Ciencia Tecnolog. 30 (2020), e2020039, https://doi.org/10.1590/0104-1428.09220.
[15] B. Nagy, C.S. Varga, K. Kontos, L. Simon-Stőger, Remarkable role of experimental olefin-maleic-anhydride copolymer based compatibilizing additives in blends of waste PET bottles and polyamide, Waste and Biomass Valorization 12 (2021) 3035–3047, https://doi.org/10.1007/s12649-020-01253-5.
[16] E. Arikan, J. Holtmannspotter, T. Hofmann, H.-J. Gudladt, Vacuum-UV of polyetheretherketone (PEEK) as a surface pre-treatment for structural adhesive bonding, J. Adhes. 96 (2018) 917–944, https://doi.org/10.1080/00218464.2018.1545646.
[17] M.J. Walzak, S. Flynn, R. Foerch, J.M. Hill, E. Karbashewski, A. Lin, M. Strobel, UV and ozone treatment of polypropylene and poly(ethylene terephthalate), J. Adhes. Sci. Technol. 9 (1995) 1229–1248, https://doi.org/10.1163/156856195X01012.
[18] M.L. Sham, J.P. Li, Cleaning and functionalization of polymer surfaces and nanoscale carbon fillers by UV/ozone treatment: a review, J. Compos. Mater. 43 (2009) 1537–1564, https://doi.org/10.1177/0021998308337740.
[19] A. Wilson, I. Jones, F. Salamat-Zadeh, J.F. Watts, Laser surface modification of poly (etheretherketone) to enhance surface free energy, wettability and adhesion, Int. J. Adhesion Adhes. 62 (2015) 69–77, https://doi.org/10.1016/j.ijadhadh.2015.06.005.
[20] S.J. Lim, J. Cheon, M. Kim, Effect of laser surface treatments on a thermoplastic PA 6/carbon composite to enhance the bonding strength, Compos. Appl. Sci. Manuf. 137 (2020) 105989, https://doi.org/10.1016/j.compositesa.2020.105989.
[21] A. Riveiro, R. Soto, R. Comesãna, M. Boutinguiza, J. del Vala, F. Quintero, F. Lusquiñnos, J. Pou, Laser surface modification of PEEK, Appl. Surf. Sci. 258 (2012) 9437–9442, https://doi.org/10.1016/j.apsusc.2012.01.154.
[22] S.W. Lee, J.W. Hong, M.Y. Wye, J.H. Kim, H.J. Kang, Y.S. Lee, Surface modification and adhesion improvement of PTFE film by ion beam irradiation, Nucl. Instrum. Methods Phys. Res. Sect. B Beam Interact. Mater. Atoms 219–220 (2004) 963–967, https://doi.org/10.1016/j.nimb.2004.01.197.
[23] P. Sundriyal, M. Pandey, S. Bhattacharya, Plasma-assisted surface alteration of industrial polymers for improved adhesive bonding, Int. J. Adhesion Adhes. 101 (2020) 102626, https://doi.org/10.1016/j.ijadhadh.2020.102626.
[24] G.D. Learn, E.J. Lai, H.A. van Recum, Nonthermal plasma treatment improves uniformity and adherence of cyclodextrin-based coatings on hydrophobic polymer substrates, Coatings 10 (2020) 1056, https://doi.org/10.3390/coatings10111056.
[25] D. Hegemann, H. Brunner, C. Oehr, Plasma treatment of polymers for surface and adhesion improvement, Nucl. Instrum. Methods Phys. Res. Sect. B Beam Interact. Mater. Atoms 208 (2003) 281–286, https://doi.org/10.1016/S0168-583X(03)00644-X.
[26] A. Khan, D. Dragatogiannis, P. Jagdale, M. Rovere, C. Rosso, A. Tagliaferro, C. Charitidis, Novel carbon fibers synthesis, plasma functionalization, and application to polymer composites, Express Polym. Lett. 15 (2021) 361–374, https://doi.org/10.3144/expresspolymlett.2021.31.
[27] S. Thomas, M. Mozetic, U. Cvelbar, P. Spatenka, K.M. Praveen (Eds.), Non-thermal Plasma Technology for Polymeric Materials. Applications in Composites, Nanostructured Materials, and Biomedical Fields, Elsevier, Amsterdam, Netherlands, 2019.
[28] J. Abenojar, R. Torregrosa-Coque, M.A. Martinez, J.M. Martin-Martinez, Surface modifications of polycarbonate (PC) and acrylonitrile butadiene styrene (ABS) copolymer by treatment with atmospheric plasma, Surf. Coating. Technol. **20**3 (2009) 2173–2180, https://doi.org/10.1016/j.surfcoat.2009.01.037.
[29] A. Kuwabara, S.-I. Kuroda, H. Kubota, Polymer surface treatment by atmospheric pressure low temperature surface discharge plasma: its characteristics and comparison with low pressure oxygen plasma treatment, Plasma Sci. Technol. 9 (2007) 181, https://doi.org/10.1088/1009-0630/9/2/14.
[30] S. Chlupová, J. Kelar, P. Slavíček, Changing the surface properties of ABS plastic by plasma, Plasma Physics and Technology 4 (2017) 32–35, https://doi.org/10.14311/ppt.2017.1.32.
[31] M. Frascio, C. Mandolfino, F. Moroni, M. Jilich, A. Lagazzo, M. Pizzorni, L. Bergonzi, C. Morano, M. Alfano, M. Avalle, Appraisal of surface preparation in adhesive bonding of additive manufactured substrates, Int. J. Adhesion Adhes. 106 (2021) 102802, https://doi.org/10.1016/j.ijadhadh.2020.102802.
[32] M.A. Martinez, J. Abenojar, S.L. de Armentia, Environmentally friendly plasma activation of acrylonitrile–butadiene–styrene and polydimethylsiloxane surfaces to improve paint adhesion, Coatings 8 (2018) 428, https://doi.org/10.3390/coatings8120428.
[33] M. Pizzorni, A. Parmiggiani, M. Prato, Adhesive bonding of a mixed short and continuous carbon-fiber-reinforced Nylon-6 composite made via fused filament fabrication, Int. J. Adhesion Adhes. 107 (2021) 102856, https://doi.org/10.1016/j.ijadhadh.2021.102856.
[34] C. Mandolfino, E. Lertora, C. Gambaro, M. Pizzorni, Durability of polyamide bonded joints: influence of surface pre-treatment, Int. J. Adhesion Adhes. 86 (2018) 123–130, https://doi.org/10.1016/j.ijadhadh.2018.08.002.
[35] P. Sauerbier, J. Anderson, D.J. Gardner, Surface preparation and treatment for large-scale 3d-printed composite tooling coating adhesion, Coatings 8 (2018) 457, https://doi.org/10.3390/coatings8120457.
[36] E. Moritzer, A. Nordmeyer, L. Enneking, A. Grishin, A. Knospe, C. Buske, Development of an Inline Plasma Treatment during Injection Molding Process, SPE ANTEC, Indianapolis, USA, 2016, pp. 1049–1054.
[37] EN ISO 4287, Geometrical product specifications (GPS), ISO 4287:1997). Surface Texture: Profile Method. Terms, Definitions and Surface Texture Parameters, 2002, p. 32.
[38] K.J. Miller, J. Savchik, A new empirical method to calculate average molecular polarizabilities, J. Am. Chem. Soc. 101 (1979) 7206–7213, https://doi.org/10.1021/ja00518a014.
[39] L. Jensen, P.-O. Astrand, A. Osted, J. Kongsten, K.V. Mikkelsen, Polarizability of molecular clusters as calculated by a dipole interaction model, J. Chem. Phys. 116 (2002) 4001–4010, https://doi.org/10.1063/1.1433747.
[40] P. Ertl, B. Rohde, P. Selzer, Fast calculation of molecular polar surface area as a sum of fragment-based contributions and its application to the prediction of drug transport properties, Journal of Medical Chemistry 43 (2000) 3714–3717, https://doi.org/10.1021/jm000942e.